Water-resonator-based metasurface : an ultrabroadband and near-unity absorption

Song, Qinghua; Zhang, Wu; Wu, Pin Chieh; Zhu, Weiming; Shen, Zhong Xiang; Chong, Peter Han Joo; Liang, Qing Xuan; Yang, Zhen Chuan; Hao, Yi Long; Cai, Hong; Zhou, Hai Feng; Gu, Yuandong; Lo, Guo-Qiang; Tsai, Din Ping; Bourouina, Tarik; Leprince-Wang, Yamin; Liu, Ai-Qun

2017

Song, Q., Zhang, W., Wu, P. C., Zhu, W., Shen, Z. X., Chong, P. H. J., . . . Liu, A.-Q. (2017). Water-resonator-based metasurface : an ultrabroadband and near-unity absorption. Advanced Optical Materials, 5(8), 1601103-. doi:10.1002/adom.201601103

https://hdl.handle.net/10356/139087

https://doi.org/10.1002/adom.201601103

DOI: 10.1002/ ((please add manuscript number))
Article type: Full Paper

Water-Resonator-Based Metasurface: An Ultra-Broadband and Near-Unity Absorption

Qinghua Song[†], Wu Zhang[†], Pin Chieh Wu, Weiming Zhu, Zhong Xiang Shen, Peter Han Joo Chong, Qing Xuan Liang, Zhen Chuan Yang, Yu Long Hao, Hong Cai, Hai Feng Zhou, Yuandong Gu, Guo-Qiang Lo, Din Ping Tsai, Tarik Bourouina, Yamin Leprince-Wang, and Ai-Qun Liu**

Q. H. Song,[†] Y. Leprince-Wang*
Université Paris-Est, ESYCOM, UPEM, F-77454 Marne-la-Vallée, France
E-mail: Yamin.Leprince@u-pem.fr

Q. H. Song, W. Zhang,[†] P. C. Wu, Z. X. Shen, P. H. J. Chong, A. Q. Liu*
School of Electrical and Electronic Engineering, Nanyang Technological University, Singapore 639798
E-mail: eaqliu@ntu.edu.sg

W. Zhang
School of Engineering and Applied Sciences, Harvard University, Massachusetts 02138, USA

W. M. Zhu
Singapore Institute of Manufacturing Technology, 71 Nanyang Drive, Singapore 638075

Q. X. Liang
School of Mechanical Engineering, Xi'an Jiaotong University, Xi'an 710049, China

Z. C. Yang, Y. L. Hao, A. Q. Liu
National Key Laboratory of Science and Technology on Micro/Nano Fabrication, Institute of Microelectronics, Peking University, Beijing 100871, China

H. Cai, H. F. Zhou, Y. D. Gu, G. Q. Lo
Institute of Microelectronics, A*STAR, Singapore 117685

D. P. Tsai
Research Center for Applied Sciences, Academia Sinica, Taipei 11529, Taiwan

T. Bourouina
Université Paris-Est, ESYCOM, ESIEE, F-93162 Noisy-le-Grand, France

[†] These authors contributed equally to this work.

Keywords: metasurface, tunable absorption, absorption material

ABSTRACT

Metasurface absorbing material, which obtains near-unity EM absorption through subwavelength artificial structure, plays an important role in the area of stealth and shielding technology, biological imaging, etc. However, they usually suffer from narrow bandwidth and only work on planar surfaces. Here, for the first time, we demonstrate a soft water-resonator-based metasurface, which functions as an active absorbing material across an ultra-broadband range of Ku, K and Ka bands. Distinct from conventional metallic metasurface, the water-resonator-based metasurface absorbs the microwave by dielectric magnetic resonance and periodic grating effect, which has a perfect absorptivity of ~99% and an absorption bandwidth (absorptivity higher than 90%) that covers 78.9% of the central frequency. Furthermore, near-unity absorption is maintained when the soft metasurface material is bent into different curvatures, promising high potential applications for antennas in reducing side lobe radiation, eliminating wall reflection in anechoic chambers, anti-radar detection and stealth.

1. Introduction

Electromagnetic (EM) absorbing material efficiently absorbs the incident electromagnetic wave, which has potential applications in EM energy harvesting,[1] bolometer,[2,3] sensor,[4] imaging system,[5] etc. In the past decade, an artificial subwavelength metallic structure array has been introduced on a metallic film separated by a dielectric layer to significantly absorb the incident light at certain frequencies, which is called perfect metamaterial/metasurface absorber (PMA).[6-10] The impedance match at the interface between PMA and free space as well as the elimination of transmission play key roles for the realization of perfect absorption. Many efforts in PMA have been focused on the metallic structure design to optimize the impedance match through plasmonic resonance,[11-15] which inevitably suffers from narrow bandwidth limitation due to high resonance dispersion. In order to broaden the absorption bandwidth, multi-band plasmonic resonances are blending together to achieve broadband absorption.[16-18] However, it is lack of tunability due to the complicated design of the metallic structure. Alternatively, dielectric metasurface, in which the optical properties can be controlled by tailoring the dielectric structure rather than metallic structure,[19,20] could also be used to control the effective impedance. One has proved that all dielectric structures can support a broad bandwidth of negtive permeability only if the dielectric losses reach a sufficiently high level.[21] On the other hand, in microwave range, the absorption of electromagnetic wave by PMAs is mainly attributed to the dielectric (volume) loss in comparison to the Ohmic (surface) loss of metal structure.[6,22] Therefore, high lossy dielectric metasurface, in which the EM wave is well confined, could also be a good candidate for perfect absorption.[23,24] In most dielectric metasurfaces,[25-32] the dielectric loss is relatively low at the operating frequencies, which hampers its applications in EM absorption. To achieve near-unity absorption, large dielectric loss in the dielectric metasurface is usually preferred. For example, an ultra-thin and highly absorptive dielectric film coated on metal

surface has been demonstrated to selectively absorb various frequency ranges of the incident EM wave in optical frequency based on interference effects.[33] A photonic-crystal slab doped with free carriers has been demonstrated to capture the terahertz wave.[34] However, an ultra-broadband absorbing material with large tunability still remains a challenge. Previous reported switchable metasurface absorber by integrating liquid crystals relies on the changing of the refractive index of liquid crystal as a function of applied electric field,[35,36] which has small tuning range and narrow absorption bandwidth.

Water is highly absorptive with large value of the imaginary part of permittivity ε'' in microwave regime due to the hydrogen bonded network among water molecules,[37] which makes it suitable for perfect EM wave absorption in this regime. However, the large contrast of permittivity between water and air causes the impedance mismatch of the water film to free space, creating a huge reflection of microwave at the water-air interface and deteriorating the absorption function. Water droplet array can be designed to supress the reflection for high absorption.[38] However, in the view of material functions, the lack of real-time controllability and suffering from the gravity effect by simply arranging water droplets on the substrate restrict its functionality in practical applications. Here, we introduce an active broadband absorbing material with large tuning range and near-unity absorption using a simple structure of water-resonator array, which is called water-resonator-based metasurface. The water-resonator-based metasurface is also actively tunable across Ku, K and Ka bands by changing the height of the water-resonator using a microfluidic control system[39,40], which not only overcomes the gravity effect, but also offers dynamic manipulation of the impedance at will. Furthermore, the water-resonator-based metasurface is a soft material, which can be bent into a large curvature to transform into various shaped structures.

2. Design of Water-Resonator-Based Metasurface

The water-resonator-based metasurface is illustrated in **Figure 1**a and the dimension of each single element is indicated in **Figure S1**. The element consists of a water sphere cap sandwiched between a top polydimethylsiloxane (PDMS) membrane and a bottom PDMS space layer with the backside being bonded to a metallic layer. A 100 μm deep circular reservoir connected with microchannel is created in the top PDMS membrane. When water is injected into the reservoir, the membrane is expanded and formed a water sphere cap due to the water pressure. The water sphere cap embedded in PDMS behaves as a resonator, which can change the impedance of the metasurface by inducing a magnetic resonance. By appropriately designing the shape of the water-resonator, the impedance of the metasurface can be trailored to match with the one of free space. Together with total reflection from the metallic reflector underneath the bottom PDMS layer, the incident EM wave energy is completely absorbed by the high lossy water-resonator and thus, near-unity absorption is realized. By changing the water volume, the top PDMS membrane can be expanded or contracted, resulting in a reversible process to flexibly reconfigure the height of the water resonator as shown in **Figure 1**b and **1**c, which enables the dynamical control of the impedance as well as the absorption spectrum. The water-resonator-based metasurface can be bent into different radii of curvature R with a fixed sample length s due to the softness of water and PDMS as shown in **Figure 1**d.

3. Numerical Analysis

The water-resonator is embeded in the low permittivity dielectric material, PDMS,[41] forming a PDMS/water/PDMS sandwich structure. The complex permittivity of water is presented in **Figure S2**. With the high ε value of water and specific geometric parameter, a magnetic

resonance and a diffraction grating effect can be excited at certain frequencies in the water-resonator. Meanwhile, the high ε'' value of water in a wide frequency range enables a broadband absorption around resonance frequencies. The calculated impedance $Z(\omega)$ by the *S*-parameter (details of simulation method is discussed in Supporting Information) when the height of the water-resonator h = 1.6 mm is shown in **Figure 2**a. At f_1 = 13.1 GHz and f_2 = 36.9 GHz, the real impedance Z' is approaching unity ($Z' \sim 1$) and the imaginary impedance Z'' is minimized to nearly zero ($Z'' \sim 0$) such that the reflection can be suppressed to nearly zero. The simulated results of the absorption spectrum is shown in **Figure 2**b. Two absorption peaks are observed at the frequency f_1 = 13.1 GHz with near-unity absorption of 98% and f_2 = 36.9 GHz with near-unity absorption of 99%, which matches well to the prediction from impedance calculation. The first absorption peak is attributed to the induced magnetic resonance mode, which can be examined by the current flow and field distribution in **Figure 2**(c-e). A circular current flow is induced at f_1 and a strong magnetic field is observed in the water-resonator as shown in **Figure 2**(c-d), respectively. Therefore, the incident microwave energy is strongly confined and absorbed in the lossy water-resonators. The typical quadrupole profile of the electric field distribution in **Figure 2**e also confirms the magnetic dipolar response. The second absorption peak is attributed to the grating effect.[42,43] The periodic water-resonator structure behaves as a 2D grating, which excites spoof surface plasmon polaritons (SPPs) at the interface between the dielectric layer and metal ground as shown in **Figure 2**f. Due to the excitation of the spoof SPPs, the incident microwave is strongly confined in the water-resonator-based metasurface as shown in the magnetic and electric field distribution in **Figure 2**(g, h). In such a case, the incident microwave can be fully absorbed by the water-resonator-based metasurface.

4. Results and Discussions

4.1 Material Fabrication

The water-resonator-based metasurface consists of 25 × 25 elements with a 5.5-mm period and the total footprint of the absorbing material is 137.5 mm × 137.5 mm. **Figure 3** shows the fabricated metasurface in which the water is injected into the water reservoirs with different volumes. The top PDMS membrane is expanded to various extents by changing the injected water volume, leading to a controllable height of the water resonator from h = 0.4 mm to 1.6 mm as shown in **Figure 3**(a-b). The water-resonator-based metasurface can be bent into an arbitrary curved surface due to the flexibility of the water and PDMS as shown in **Figure 3**c. The water-resonators are confined in the water reservoirs formed by two PDMS layers, which can minimize the gravitational effect on water-resonators. In the following experiment, the water-resonator-based metasurface sample is fixed vertically.

4.2 Measurement of Ultra-Broadband Absorption

The absorption properties of the water-resonator-based metasurface are first investigated by changing the height of the water resonators. The absorption peak at the lower frequency shows a red shift from K band (20 GHz) to Ku band (15 GHz) when the height of the water-resonator is increased from 0.4 mm to 1.2 mm as shown in **Figure 4**, because the effective length of the magnetic resonance is increased. On the other hand, the absorption peak at the higher frequency is not shifted because it is caused by grating effect from the periodic resonator array. As a result, the bandwidth of absorption is tuned by both magnetic resonance and grating effect when the water-resonator height is changed. The tunable broadband absorption is simulated and experimentally demonstrated as shown in **Figures 4**a and b, respectively, which realizes a maximum absorption of 99%. When the height of the water-

resonator is 0.4 mm, the absorption bandwidth of the central frequency is 78.5% and 78.9% with over 90% absorption in the simulation and experimental results, respectively. The mismatch of the bandwidth is less than 2% between the experimental and simulation results, which is induced by the fabrication error. Each water-resonator are not uniform due to the inhomogeneous pressure in the water reservoir. These non-monodispersed water-resonators affects the bandwidth of the absorption. To demonstrate that the microwave is indeed absorbed by the metasurface but not scattered to other directions, measurements at different reflected angles are shown and explained in **Figure S3**.

4.3 Wide Incident Angle

The water-resonator-based metasurface is also demonstrated to realize a wide incident angle absorption in a broad bandwidth. **Figure 5** shows the measured absorption spectra of the metasurface under both TE and TM polarization incidence while the height of the water resonator keeps at 0.4 mm. The absorption bandwidth keeps at about 66.7% related to the central frequency with the absorption level higher than 80%. With the presence of the water channels, the absorption is slightly different for TE and TM mode in normal incidence at high frequency due to the polarization dependence of magnetic resonance and grating effect, which is consistent with the simulation results as shown in **Figure S4**. The large incident angle broadband absorption of water-resonator-based metasurface could promises an omnidirectional broadband absorption on arbitrary curved surfaces.

4.4 Omnidirectional Absorption on Curved Surfaces

When a curved surface is illuminated by a plane wave, the reflective wave will scatter into different directions. Due to the large-angle absorption and high flexibility of soft water-

resonator-based metasurface, an omnidirectional absorbing material is demonstrated when the water-resonator-based metasurface is bent, whereby both the specular reflective wave and the abnormal scattering wave are suppressed under normal illumination. Here, omnidirectional absorption means no reflection/scattering is observed in all directions when the microwave is normally incident on the metasurface. The omnidirectional broadband absorption of the curved metasurface absorption functional material is characterized and compared with the absorption of a bare metal curved surface with the same curvature. **Figure 6**a shows the reflection spectra of a bare metal curved surface with a small curvature of R = 200 mm and s = 130 mm. High reflectance is detected at all directions from $\varphi = 0^{o}$ to $\varphi = 75^{o}$ (each step size of 15^{o}), where φ is the azimuth angle of the detector position. When the metal curved surface is covered by the water-resonator-based metasurface (h = 0.4 mm), the reflection to all directions is significantly suppressed to almost zero from 20 to 40 GHz as shown in **Figure 6**b. Similar results are observed when the metal curved surface is bent to a larger curvature of R = 100 mm. The reflectance (**Figure 6**c) from $\varphi = 0^{o}$ to $\varphi = 75^{o}$ is suppressed to negligible level with the cover of water-resonator-based metasurface as shown in **Figure 6**d. As a result, an omnidirectional and ultra-broadband absorption functional material on different curved surfaces is achieved with a bandwidth of 66.7% from 20 GHz to 40 GHz.

4.5 Broadband Intensity Modulation

Besides a perfect absorption, controllable absorptivity is also demanded in many potential applications. The water-resonator-based metasurface provides a very convenient approach to control the absorptivity by simply replacing water with other different dielectric constant liquids. In the experiment, we inject ethanol solutions with different concentrations to change the absorptivity of the water-resonator-based metasurface. **Figure S5** shows that both the real part (ε') and imaginary part (ε'') of the effective permittivity of the mixture solution decrease

with an increased concentration of ethanol in the solution.[44] The decreasing of ε' undermines the microwave confinement in the original water-resonator, while the decreasing of ε'' further decreases the wave absorption in the metasurface. **Figure 7**a and **Figure 7**b show the simulation and experimental results of the absorption spectra with different concentrations of ethanol solutions, respectively. As expected, the absorption level decreases from about 90% to below 20% in the entire measured frequency regime, when the ethanol concentration in the solution is increased from 0% (pure water) to 100% (pure ethanol). As a result, the absorptivity of the water-resonator-based metasurface can be continuously controlled by simply injecting ethanol solution with the corresponding concentration.

5. Conclusions

In conclusion, for the first time, an embedded water-resonator-based metasurface with broadband absorption across the entire Ku, K and Ka bands is demonstrated. The water-resonator-based metasurface induces a strong magnetic resonance, which incorporates with the grating effect, to achieve the impedance matching to free space in broad bandwidth. By controlling the water injection in the PDMS microchannel, the absorption band is tuned through different heights of the water-resonators. The bandwidth of the central frequency of the metasurface reaches 78.9% with higher than 90% absorption under normal incident microwave. The high absorption and large bandwidth are also preserved with oblique incidence from 0º to 45º. In addition, an omnidirectional and broadband absorbing material is realized by the curved soft metasurface. Finally, a broadband intensity modulation is demonstrated by injecting different concentrations of ethanol solution. The metasurface absorbing material has high potential applications for antennas in reducing side lobe radiation, eliminating wall reflection in anechoic chambers, anti-radar detection and stealth technology.

6. Experimental Setup

The fabrication processes of the water-resonator-based metasurface is illustrated in **Figure S6**. Measurement setup for **Figure 4**, **Figure 5** and **Figure 7** is shown in **Figure S7**a. Two dual-polarized quadruple-ridged horns serve as the source and receiver, respectively. The source (tinted in red) can move along the left arc with an incident angle of φ_i. On the other hand, the receiver (tinted in green) can move along the right arc with a reflective angle of $\varphi_r = \varphi_i$. Measurement setup for **Figure 6** is shown in **Figure S7**b. The source is fixed at the incident angle of 0° in a holder. The incident wave is assumed as a plane wave. The receiver direction $\varphi_r' = \varphi_i'$. The contact point of the source antenna extension line and the sample is represented as A, while the contact point of the receiver extension line and the sample is represented as B_n. The arc length of AB_n is defined as S_n. In the measurement, the position of B_n is chosen as $S_n = 10n$ mm (n = 0, 1, 2 ⋯ 6). Both horns (source and receiver) are placed 1.2 m away from the sample and connected to a vector network analyzer (VNA, Agilent N4693A) in order to characterize the far-field reflection properties.

Supporting Information

Supporting Information is available from the Wiley Online Library or from the author.

Acknowledgement

The authors acknowledge F. Capasso and N. I. Zheludev for the useful discussions and valuable suggestions.
The work is mainly supported by National Research Foundation, Singapore (NRF-CRP13-2014-01); Ministry of Education (MOE), Singapore (Tier-1 RG89/13); and Economic Development Board, Singapore (NRF2014SAS-SRP001-059).
Q. H. Song and W. Zhang contributed equally to this work.

Received: ((will be filled in by the editorial staff))
Revised: ((will be filled in by the editorial staff))
Published online: ((will be filled in by the editorial staff))

References

[1] C. F. Guo, T. Sun, F. Cao, Q. Liu, Z. Ren, *Light Sci. Appl.* **2014**, 3, e161.

[2] F. B. P. Niesler, J. K. Gansel, S. Fischbach, M. Wegener, *Appl. Phys. Lett.* **2012**, 100, 203508.

[3] T. Maier, H. Brückl, *Opt. Lett.* **2009**, 34, 3012-3014.

[4] N. Liu, M. Mesch, T. Weiss, M. Hentschel, H. Giessen, *Nano Lett.* **2010**, 10, 2342-2348.

[5] C. M. Watts, D. Shrekenhamer, J. Montoya, G. Lipworth, J. Hunt, T. Sleasman, S. Krishna, D. R. Smith, W. J. Padilla, *Nature Photon.* **2014**, 8, 605-609.

[6] N. Landy, S. Sajuyigbe, J. Mock, D. Smith, W. Padilla, *Phys. Rev. Lett.* **2008**, 100, 207402.

[7] C. M. Watts, X. Liu, W. J. Padilla, *Adv. Mater.* **2012**, 24, OP98-OP120.

[8] J. Rhee, Y. Yoo, K. Kim, Y. Kim, Y. Lee, *J. Electromagnet. Wave* **2014**, 28, 1541-1580.

[9] G. Sun, C. T. Chan, *Phys. Rev. E Stat. Nonlin. Soft Matter Phys.* **2006**, 73, 036613.

[10] J. Ng, H. Chen, C. T. Chan, *Opt. Lett.* **2009**, 34, 644-646.

[11] H. Tao, C. Bingham, D. Pilon, K. Fan, A. Strikwerda, D. Shrekenhamer, W. Padilla, X. Zhang, R. Averitt, *Journal of physics D: Applied physics* **2010**, 43, 225102.

[12] J. W. Park, P. Van Tuong, J. Y. Rhee, K. W. Kim, W. H. Jang, E. H. Choi, L. Y. Chen, Y. Lee, *Opt. Express* **2013**, 21, 9691-9702.

[13] Y. J. Yoo, Y. J. Kim, P. Van Tuong, J. Y. Rhee, K. W. Kim, W. H. Jang, Y. Kim, H. Cheong, Y. Lee, *Opt. Express* **2013**, 21, 32484-32490.

[14] P. V. Tuong, J. W. Park, J. Y. Rhee, K. W. Kim, W. H. Jang, H. Cheong, Y. P. Lee, *Appl. Phys. Lett.* **2013**, 102, 081122.

[15] X. Shen, Y. Yang, Y. Zang, J. Gu, J. Han, W. Zhang, T. J. Cui, *Appl. Phys. Lett.* **2012**, 101, 154102.

[16] F. Ding, Y. Cui, X. Ge, Y. Jin, S. He, *Appl. Phys. Lett.* **2012**, 100, 103506.

[17] Y. Cui, K. H. Fung, J. Xu, H. Ma, Y. Jin, S. He, N. X. Fang, *Nano Lett.* **2012**, 12, 1443-1447.

[18] A. K. Azad, W. J. M. Kort-Kamp, M. Sykora, N. R. Weisse-Bernstein, T. S. Luk, A. J. Taylor, D. A. R. Dalvit, H. T. Chen, *Sci. Rep.* **2016**, 6, 20347.

[19] Y. Yang, I. I. Kravchenko, D. P. Briggs, J. Valentine, *Nat. Commun.* **2014**, 5, 5753.

[20] D. Lin, P. Fan, E. Hasman, M. L. Brongersma, *Science* **2014**, 345, 298-302.

[21] R. Yahiaoui, H. Němec, P. Kužel, F. Kadlec, C. Kadlec, P. Mounaix, *Opt. Lett.* **2009**, 34, 3541-3543.

[22] J. E. Raynolds, B. A. Munk, J. B. Pryor, R. J. Marhefka, *J. Appl. Phys.* **2003**, 93, 5346-5358.

[23] R. Kakimi, M. Fujita, M. Nagai, M. Ashida, T. Nagatsuma, *Nature Photon.* **2014**, 8, 657-663.

[24] S. J. Kim, P. Fan, J. H. Kang, M. L. Brongersma, *Nature Commun.* **2015**, 6, 7591.

[25] M. Khorasaninejad, F. Aieta, P. Kanhaiya, M. A. Kats, P. Genevet, D. Rousso, F. Capasso, *Nano Lett.* **2015**, 15, 5358-5362.

[26] F. Aieta, M. A. Kats, P. Genevet, F. Capasso, *Science* **2015**, 347, 1342-1345.

[27] A. E. Krasnok, A. E. Miroshnichenko, P. A. Belov, Y. S. Kivshar, *Opt. Express* **2012**, 20, 20599-20604.

[28] D. Lin, P. Fan, E. Hasman, M. L. Brongersma, *Science* **2014**, 345, 298-302.

[29] A. E. Miroshnichenko, Y. S. Kivshar, *Nano Lett.* **2012**, 12, 6459-6463.

[30] M. V. Rybin, D. S. Filonov, K. B. Samusev, P. A. Belov, Y. S. Kivshar, M. F. Limonov, *Nature Commun.* **2015**, 6, 10102.

[31] A. Arbabi, Y. Horie, A. J. Ball, M. Bagheri, A. Faraon, *Nature Commun.* **2015**, 6, 7069.

[32] A. Andryieuski, S. M. Kuznetsova, S. V. Zhukovsky, Y. S. Kivshar, A. V. Lavrinenko, *Sci. Rep.* **2015**, 5.

[33] M. A. Kats, R. Blanchard, P. Genevet, F. Capasso, *Nature Mater.* **2013**, 12, 20-24.

[34] R. Kakimi, M. Fujita, M. Nagai, M. Ashida, T. Nagatsuma, *Nat. Photonics*, **2014**, 8, 657-663.

[35] D. Shrekenhamer, W. C. Chen, W. J. Padilla, *Phys. Rev. Lett.* **2013**, 110, 177403.

[36] S. Savo, D. Shrekenhamer, W. J. Padilla, *Adv. Opt. Mater.* **2014**, 2, 275-279.

[37] R. Buchner, J. Barthel, J. Stauber, *Chem. Phys. Lett.* **1999**, 306, 57-63.

[38] Y. J. Yoo, S. Ju, S. Y. Park, Y. Ju Kim, J. Bong, T. Lim, K. W. Kim, J. Y. Rhee, Y. P. Lee, *Sci. Rep.* **2015**, 5, 14018.

[39] W. Zhu, Q. Song, L. Yan, W. Zhang, P. C. Wu, L. K. Chin, H. Cai, D. P. Tsai, Z. X. Shen, T. W. Deng, *Adv. Mater.* **2015**, 27, 4739-4743.

[40] H. Zhao, Y. Yang, L. Chin, H. Chen, W. Zhu, J. Zhang, P. Yap, B. Liedberg, K. Wang, G. Wang, *Lab on a Chip* **2016**, 16, 1617-1624.

[41] J. C. Booth, N. D. Orloff, J. Mateu, M. Janezic, M. Rinehart, J. A. Beall, *IEEE T. Instrum. Meas.* **2010**, 59, 3279-3288.

[42] Y. Qu, Q. Li, H. Gong, K. Du, S. Bai, D. Zhao, H. Ye, M. Qiu, *Adv. Opt. Mater.* **2016**, 4, 480-486.

[43] M. Pu, M. Wang, C. Hu, C. Huang, Z. Zhao, Y. Wang, X. Luo, *Opt. Express* **2012**, 20, 25513-25519.

[44] Y. W. Afsar, *Prog. Electromagn. Res.* **2003**, 42, 131-142.

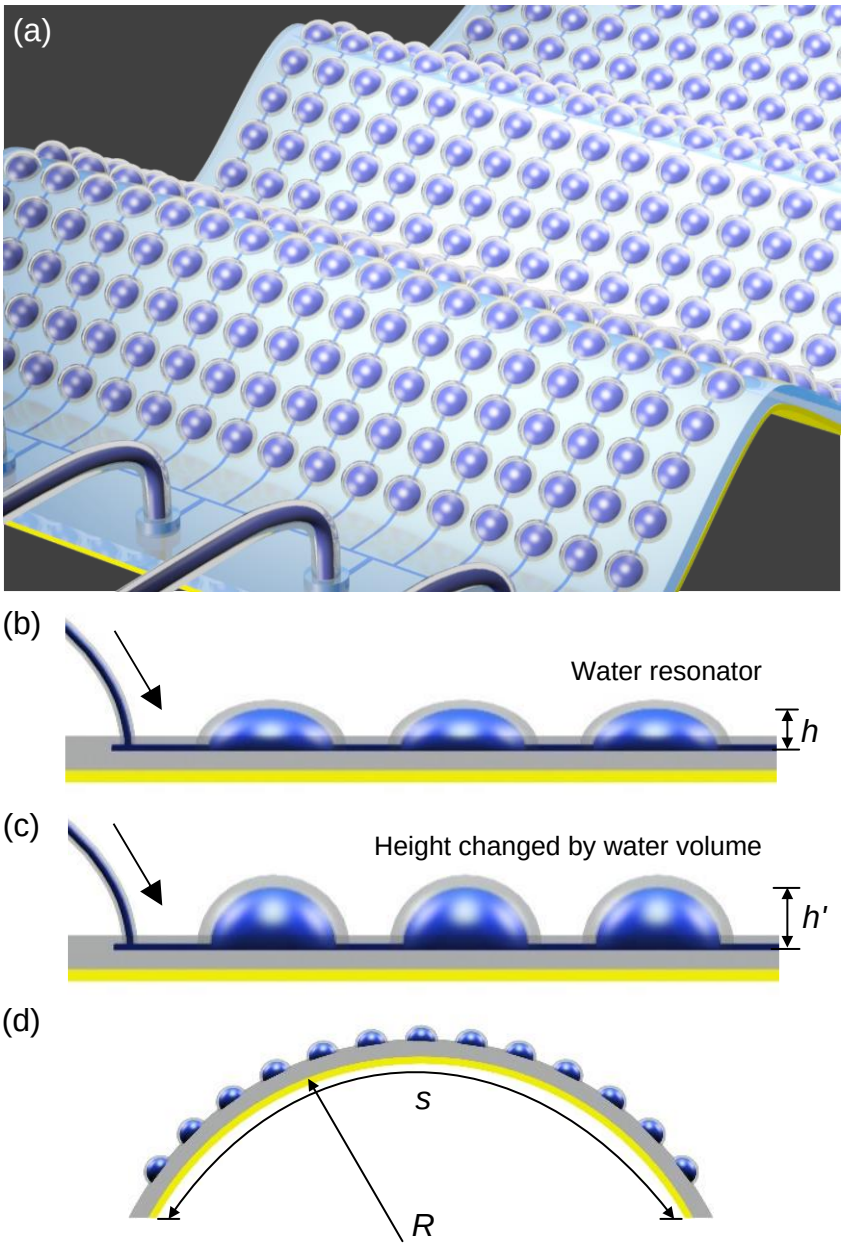

Figure 1. Schematic of water-resonator-based metasurface. (a) Water-resonator-based metasurface consists of a top PDMS membrane layer and a bottom PDMS-metallic layer. (b) Side view of the embeded water-resonators with water injection. (c) Height of water-resonator is actively tuned by different water volumes. (d) Soft metasurface absorption functional material is bent to arbitrary curvature.

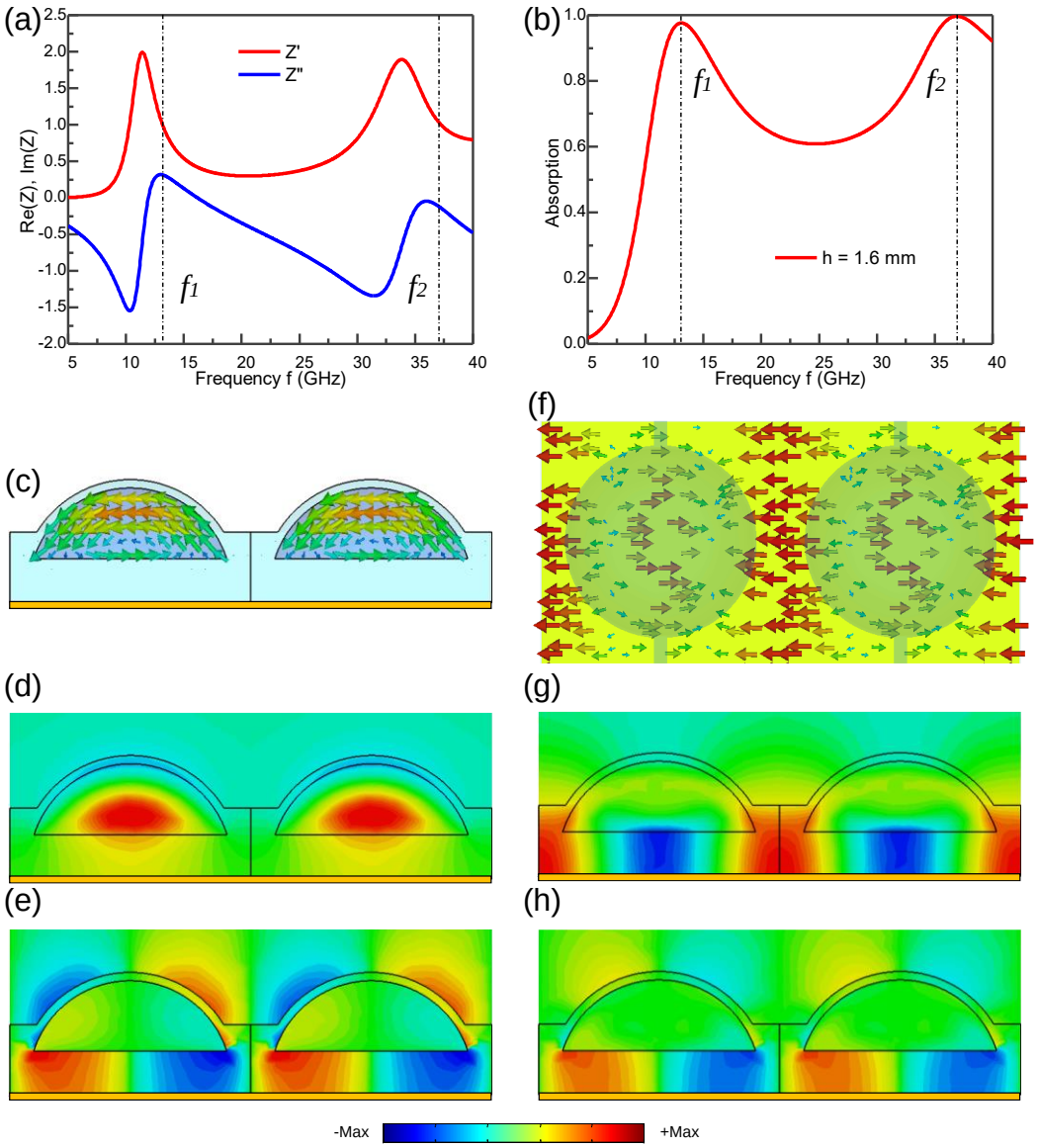

Figure 2. Simulation results when height of water-resonator *h* = 1.6 mm. (a) Calculated impedance of water-resonator-based metasurface retrieved from *S*-parameter. (b) Absorption of the water resonator-based metasurface. Side view of (c) current density, (d) magnetic distribution H_x and (e) electric distribution E_z at the absorption peak f_1. Top view of (f) surface current of the metal ground plane; side view of (g) magnetic distribution H_x and (h) electric distribution E_z at the absorption peak f_2. Scale bar presents the field amplitude for (d, e, g, h).

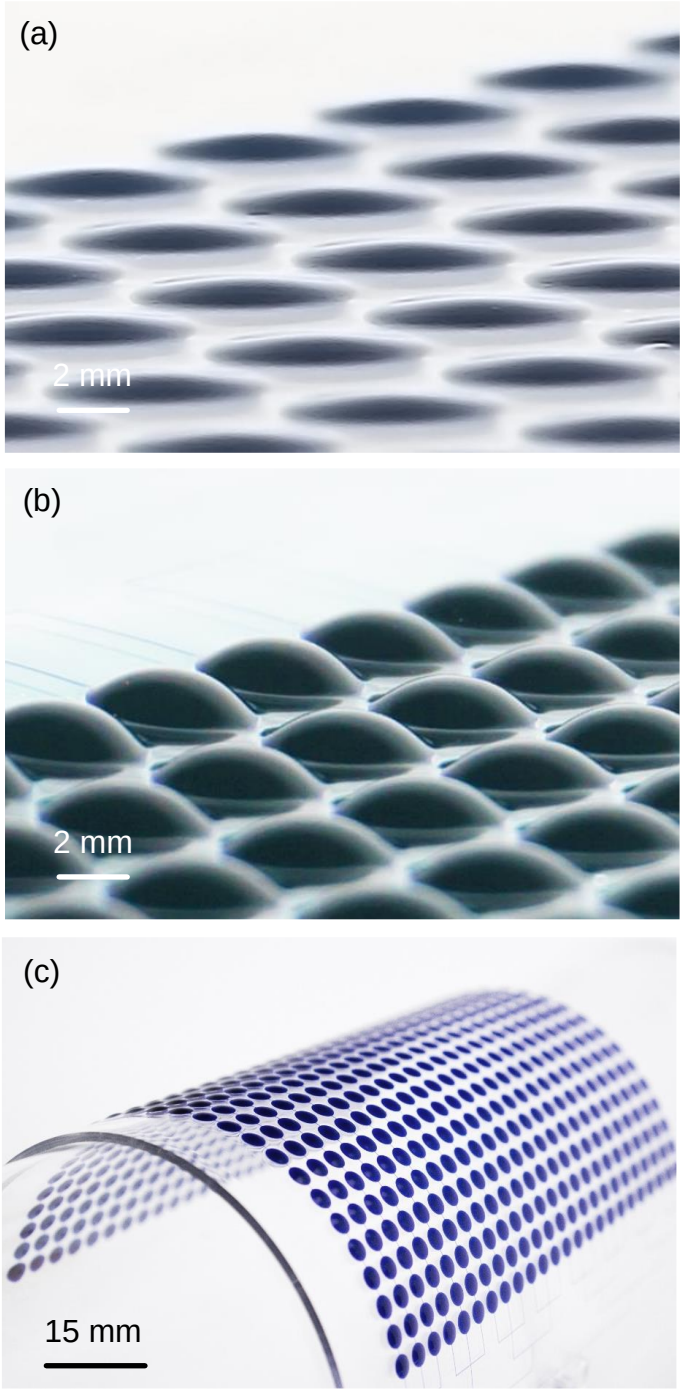

Figure 3. Photographs of water-resonator-based metasurface. (a) Water is injected into the PDMS with height of h = 0.4 mm. (b) Height of water-resonator is increased to h = 1.6 mm by increasing the water volume. (c) Water-resonator-based metasurface is bent to an arbitrary curvature.

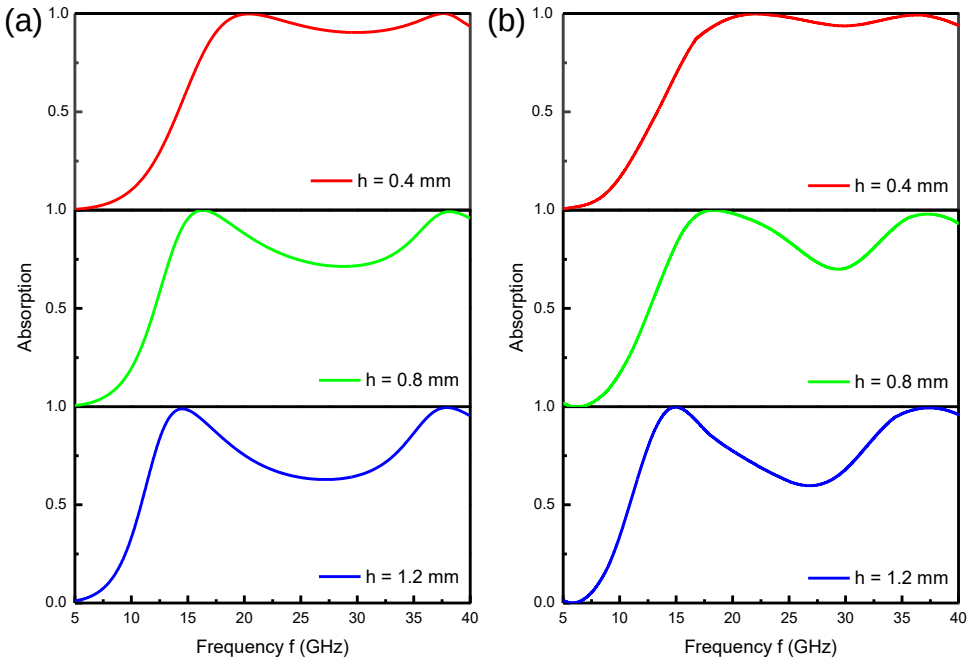

Figure 4. Absorption spectra with different heights of water-resonators. (a) Simulation and (b) experimental results of the absorption spectrum when the height of the water-resonator is changed from 0.4 mm to 0.8 mm and 1.2 mm.

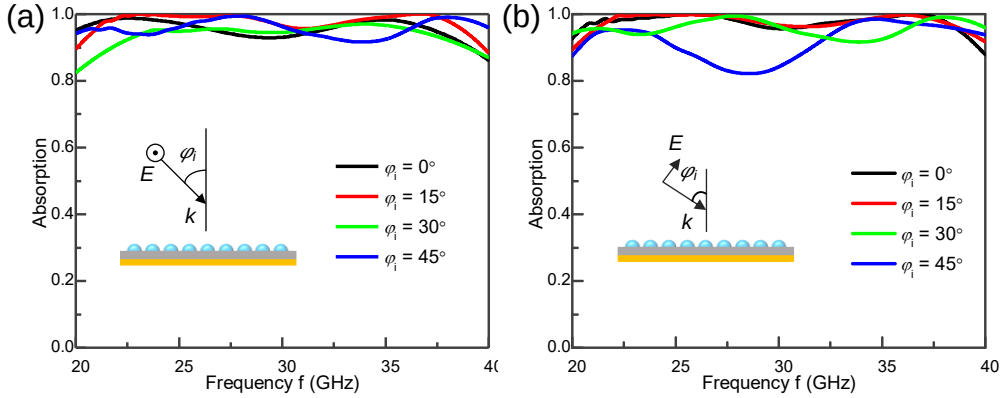

Figure 5. A broadband absorbing material with wide incident angle. Measured absorption spectra with (a) TE mode and (b) TM mode, respectively, by changing the incident angle from 0º to 45º. Height of the water-resonator is 0.4 mm.

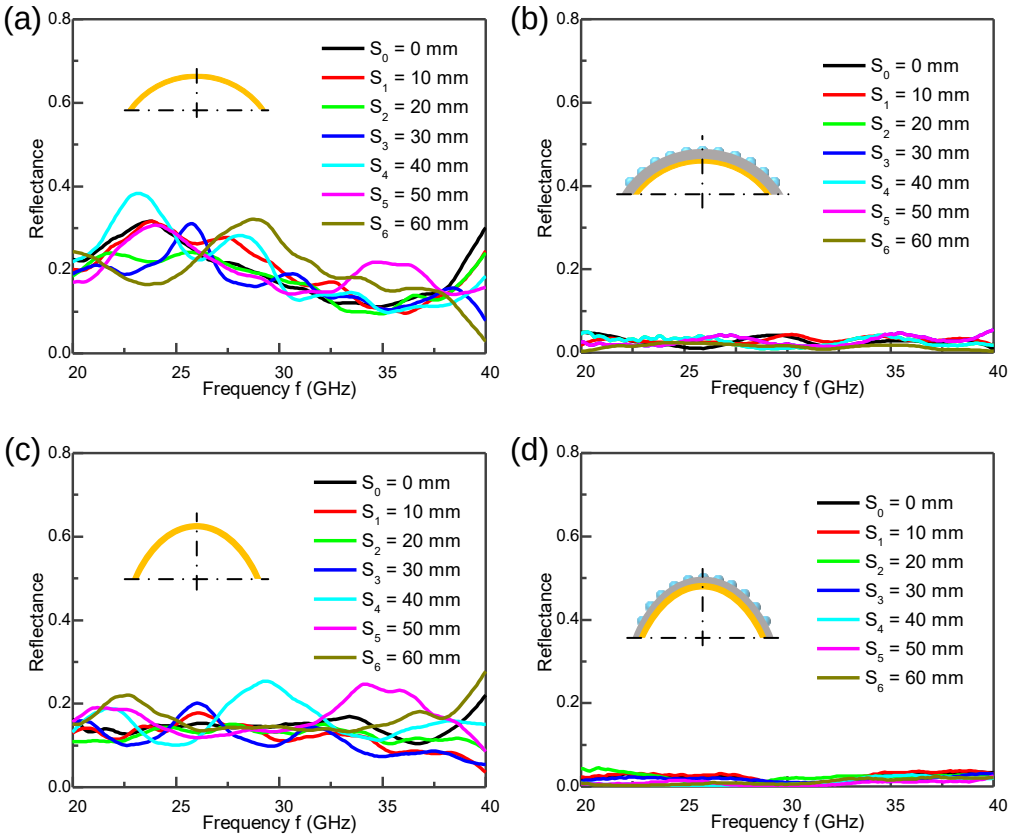

Figure 6. An omnidirectional broadband absorbing material on curved surface. (a, b) Reflectance spectrum at different reflective positions (see **Figure S7**) of a bare metal curved surface and the curved water-resonator-based metasurface when the curvature is small (R = 200 mm), respectively. (c, d) Reflectance spectrum at different reflective angles of a bare metal curved surface and the curved water-resonator-based metasurface when the curvature is increased (R = 100 mm), respectively.

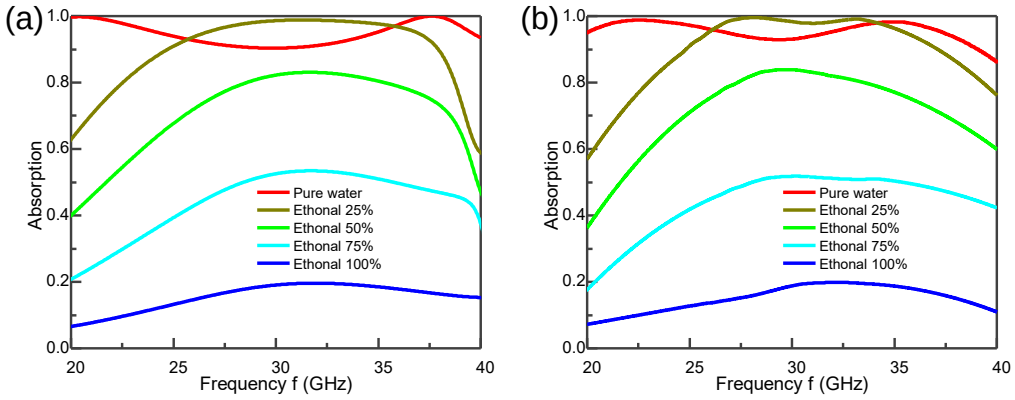

Figure 7. Broadband intensity modulation with different concentrations of ethanol solution. (a) Simulation and (b) experimental results of the absorption spectra with different concentration of ethanol solution. Height of the water-resonator is 0.4 mm.